Article

Not peer-reviewed version

Microstrip MIMO Antennas for High-Band in 5G Systems

Marek Bugaj *, Rafał Przesmycki, Kuba Bugaj

Posted Date: 25 March 2026

doi: 10.20944/preprints202603.1927.v1

Keywords: antenna; microstrip antenna; MIMO; CST Studio; 5G system; high-band 38 GHz

 doi:10.20944/preprints202603.1927.v1

Article

Microstrip MIMO Antennas for High-Band in 5G Systems

Marek Bugaj *, Rafał Przesmycki and Kuba Bugaj

Military University of Technology, 00-908 Warsaw, Poland, Gen. Sylwestra Kaliskiego 2 str.

* Correspondence: marek.bugaj@wat.edu.pl; Tel.: +48-261-83-78-85

Abstract

This article presents the design and analysis of microstrip MIMO antennas intended for operation in the 5G high-frequency band (High-Band). The proposed antenna structures include 2 and 4 element MIMO configurations operating in the millimeter-wave spectrum with a center frequency of 38 GHz. The aim of the article was to develop compact antenna systems with performance parameters suitable for 5G mmWave applications, while addressing the limitations of microstrip technology. This article describes the development process of a single radiating element and its subsequent integration into multi-antenna structures. Particular attention is paid to impedance matching, port isolation, and mutual coupling mitigation, which represent key challenges in implementing MIMO antennas within the millimeter-wave band. Furthermore, the impact of the number of antenna elements on the radiation pattern, gain, and overall efficiency of the MIMO system is analyzed. The obtained results confirm that MIMO microstrip antennas in 2- and 4-element configurations can be an effective solution for 5G High-Band applications, providing adequate radio parameters while maintaining small dimensions and the ability to integrate with RF front-end systems. The presented solutions can be used in user terminals, CPE modules, and compact access stations of 5G systems operating in the millimeter-wave band.

Keywords: antenna; microstrip antenna; MIMO; CST Studio; 5G system; high-band 38 GHz

1. Introduction

The rapid development of fifth-generation (5G) wireless systems calls for increasingly sophisticated antenna solutions, particularly in the high-frequency band (HB), which encompasses millimeter waves. One of the primary frequency ranges designated for 5G HB is centered around 38 GHz; this range enables ultra-wide bandwidths, thereby achieving exceptionally high data rates. However, operating in this band presents substantial propagation challenges, such as high free-space path loss, limited obstacle penetration, and high susceptibility to blockage, which impose stringent requirements on antenna system design.

To address these limitations, 5G systems commonly employ MIMO (Multiple Input Multiple Output) technology, which leverages multiple antenna elements to simultaneously transmit and receive radio signals. MIMO facilitates enhanced data throughput via spatial multiplexing, improves link reliability, and mitigates propagation losses through spatial diversity and beamforming. In the millimeter-wave band, this technique is particularly effective because its short wavelength allows for the integration of dense, multi-element antenna structures within the limited space of end devices and base stations.

Among the most promising solutions for mmWave applications are microstrip antennas, characterized by their low profile, lightweight nature, and ease of fabrication using printed circuit technology. They facilitate seamless integration with radio circuitry and RF front-ends, positioning them as compelling candidates for 5G High-Band modules. However, designing microstrip MIMO arrays at 38 GHz remains a complex challenge, necessitating the address of issues such as narrow

 doi:10.20944/preprints202603.1927.v1

element bandwidth, pronounced mutual coupling, and high parametric sensitivity to manufacturing tolerances.

This article presents the design and analysis of MIMO microstrip antennas in 2- and 4-element configurations, designed for operation in the high-band band of 5G technology. The presented solutions include the selection of a single radiating element geometry, the arrangement of elements in the MIMO structure, and the analysis of mutual coupling. The analysis includes both port matching and isolation parameters, as well as radiation characteristics and the potential usefulness of the designed antennas in modern 5G mmWave systems.

2. 5G and MIMO Technology

5G NR (5G New Radio) systems are designed to operate over an exceptionally wide frequency range, encompassing both sub-1 GHz bands and millimeter waves above 24 GHz. To organize the properties of these bands and the resulting opportunities and limitations, engineering practice divides the 5G band into three main areas: Low-Band, Medium-Band (Mid-Band), and High-Band (mmWave). Each of these bands is characterized by distinct propagation parameters, varying available bandwidths, and diverse hardware and antenna requirements. 5G technology facilitates the utilization of frequencies across a broad spectrum. Based on the current state of 5G network standardization and the availability of dedicated frequencies, the following frequency bands are expected to be used: Low-Band 700 MHz (694–790 MHz), Mid-Band 3.6 GHz (3.4–3.8 GHz), and High-Band 26 GHz (24.25–27.5 GHz) and 38 GHz (37 GHz–40 GHz). The maximum frequency resources in these bands are: 2 × 30 MHz (part of the band), 200 MHz, and 400 MHz, respectively. It should be emphasized that these bands are subject to harmonization in Europe and many countries around the world, meaning that mobile terminal users will be able to access 5G network services in various countries. 5G networks will utilize multiple bands simultaneously, including bands currently used by 4G systems (e.g., 1800 MHz, 2100 MHz, 2600 MHz) [1–4].

The Low-Band band covers frequencies below approximately 1 GHz, typically in the 700 to 900 MHz range. The electromagnetic wavelength in this band ranges from approximately 30 cm to 50 cm, which directly translates into very favorable propagation conditions. Free-space attenuation is relatively low, and diffraction and penetration through obstacles and building walls are significantly better than in higher bands. Typical cell radii in Low-Band can reach several, or even a dozen, kilometers, with relatively low base station transmitting power. However, from a system parameter perspective, the available bandwidth is limited—standard channels are 5–20 MHz wide. This results in a moderate maximum data rate, typically comparable to or slightly higher than in LTE networks. In practice, low-band in 5G is primarily used to provide coverage, signaling, user mobility, and services requiring high reliability but not extreme transmission speeds. Antenna configurations in this band are typically simple (2-element MIMO or 4-element MIMO), and antenna gain is limited by the physical size and shape of the radiating elements.

The Medium-Band band, also called Mid-Band, covers frequencies from approximately 1 to 6 GHz, with the ranges around 3-4 GHz playing a key role. The wavelength in this band is from a few to several centimeters, which means worse propagation properties compared to Low-Band, but still sufficient to effectively cover urban and suburban areas. Typical cell radii in Mid-Band range from several hundred meters to several kilometers, depending on transmit power, antenna height, and the propagation environment. A key advantage of Medium-Band is access to much wider frequency channels, reaching 80–100 MHz, and in some cases even more with band aggregation. This allows for significantly higher data rates and lower latency compared to low-band. Advanced MIMO techniques, such as 4-element, 8-element, and even massive MIMO at the base station level, are commonly used in this regard, increasing network capacity and spectral efficiency. Medium-band is currently the fundamental pillar of commercial 5G deployments, combining relatively good coverage with high system performance [1][5–7].

The high-band band, also known as the millimeter-wave (mmWave) band, encompasses frequencies above 24 GHz, including the ranges around 26 GHz, 28 GHz, and 38 GHz. The

 doi:10.20944/preprints202603.1927.v1

wavelengths in this band are on the order of a few millimeters, enabling the design of very compact antennas and high-density, large-scale antenna arrays. At the same time, free-space path loss increases significantly with frequency, with additional losses caused by atmospheric absorption, rainfall, and very poor obstacle penetration. In practice, the range of a single high-band cell is limited to a few dozen or several hundred meters, and the radio link requires near-line-of-sight (LOS) or carefully selected reflections. In practice, the range of a single high-band cell is limited to a few dozen or a few hundred meters, and the radio link requires near-line-of-sight (nLOS) or carefully selected reflections. The greatest advantage of this band is access to very wide frequency channels—often on the order of several hundred megahertz (e.g., 400 MHz)—enabling extremely high data rates measured in gigabits per second. To compensate for significant propagation losses, these bands require high-gain antennas, multi-element MIMO arrays, and dynamic beamforming. Antenna systems in this range are typically integrated with active systems and contain dozens or even hundreds of radiating elements [1,5–7].

From a technical perspective, the division of the 5G band into Low, Medium, and High Band reflects a fundamental compromise between the range, capacity, and throughput of the radio system. Low frequencies ensure wide coverage and connection stability, medium frequencies offer the best balance of parameters for public networks, while millimeter-wave bands enable the most demanding transmission scenarios at the expense of very limited range and high infrastructure complexity. This multi-band nature of 5G means that modern networks are designed as heterogeneous systems, in which individual bands complement each other, ensuring both continuous coverage and very high data transmission efficiency [1].

However, bandwidth alone is not sufficient to achieve the desired 5G parameters, especially under conditions of limited power budget and unfavorable propagation. For this reason, MIMO technology plays a key role, i.e., the transmission and reception of signals using multiple antennas at the transmitter and receiver. In its simplest terms, MIMO takes advantage of the fact that in a radio environment, signals reach the receiver via multiple independent paths (propagation paths), and each of these paths can carry some information. Instead of treating multipath as an undesirable phenomenon, the MIMO system uses it to increase transmission efficiency [8,9].

From a technical perspective, MIMO enables several key mechanisms. The first is spatial multiplexing, in which different data streams are transmitted simultaneously on the same frequency but using different antennas and different spatial signal characteristics. This allows for an almost proportional increase in throughput with the number of independent antenna paths, provided that propagation conditions ensure sufficiently low correlation between channels. The second mechanism is spatial diversity, which aims to improve link reliability by reducing the impact of signal fading. In this case, the same data can be transmitted by multiple antennas, and the receiver selects or combines the signals to ensure the highest reception quality. The third aspect is beamforming, which shapes the antenna radiation pattern so that energy is directed towards a specific user, improving the signal-to-noise ratio and increasing the effective range of the link.

The implementation of MIMO in 5G addresses several fundamental limitations of radio systems. First, since the frequency spectrum is a finite resource, increasing throughput solely through bandwidth expansion is not always feasible. MIMO enhances spectral efficiency, maximizing the data rate transmitted per unit of bandwidth. Second, in higher frequency bands where propagation losses are severe, beamforming implemented via MIMO architectures allows for their effective mitigation. Third, in high-density environments, MIMO enables the simultaneous support of multiple terminals (Multi-User MIMO), significantly improving network capacity and Quality of Service (QoS) [10,11].

In summary, 5G technology represents a significant step forward in the development of wireless systems, and MIMO is one of its key pillars. By leveraging multiple antennas and the spatial properties of the radio channel, it is possible to significantly increase data throughput, improve connection reliability, and efficiently utilize the available frequency spectrum. Combined with wide frequency bands, flexible signal structure, and advanced network architecture, MIMO enables the

 doi:10.20944/preprints202603.1927.v1

implementation of 5G objectives in both low- and mid-frequency bands and the challenging propagation conditions of the millimeter-wave band.

3. MIMO Microstrip Antennas for 5G High-Band

MIMO (Multiple-Input Multiple-Output) antennas in 2- and 4-element configurations are primarily used in 5G systems to increase the throughput and reliability of the radio link. In the high-band (mmWave) band—such as 38 GHz—energy gain and directivity become critical because free-space attenuation increases with frequency, and the signal is also highly sensitive to overshadowing. For this reason, a typical solution combines two ideas: (1) multiple MIMO paths to achieve capacitive gain and fade immunity, and (2) a small, flat microstrip antenna that is easily integrated with the radio module and a phasing/beamforming system. In practice, "2-element MIMO" means two independent radiating ports (two elements or two polarization/geometrically separated radiators), while "4-element MIMO" means four ports, which gives greater spatial flexibility (more degrees of freedom of the channel) and the possibility of obtaining a higher bit rate or a more stable link at the same transmit power [12–14].

Microstrip technology most often uses a rectangular patch on a low-loss laminate, above the ground plane, with a microstrip or coaxial line supply. For 38 GHz, reducing dielectric and conduction losses is crucial, so substrates with low loss tangent (e.g., RF/microwave class) and the lowest possible copper roughness are selected. Isolation between ports (low coupling coefficient $|S_{21}|$) is also important from a MIMO perspective, as strong coupling reduces effective channel independence, worsens the envelope correlation coefficient (ECC), and consequently limits MIMO gain. In the 38 GHz band, typical distances between elements are of the order of a fraction of a wavelength, i.e., several millimeters, which makes the problem of isolation and integration particularly important—spatial separation, orthogonal polarization, corner elements, ground gaps or neutralizing line segments are often used [15,16].

The starting point for the computational partis the design of a single element—a resonant patch at 38 GHz—followed by the construction of 2- and 4-element configurations. This approach allows for evaluating the impact of geometry on gain, beamwidth, and coupling. For the purpose of these simulations, a center frequency of f0=38 GHz is assumed. The wavelength in a vacuum is $\lambda_0 = \frac{c}{f_0}$, where $c \approx 3 \cdot 10^8$ m/s, therefore $\lambda_0 \approx \frac{3 \cdot 10^8}{38 \cdot 10^9} \approx 7{,}89$ mm. In a microstrip antenna, the electromagnetic wave propagates through a combination of the dielectric substrate and the surrounding air. Consequently, the wave 'sees' an effective permittivity (εeff), which is lower than the substrate's relative permittivity. This results in an effective wavelength within the structure that is shorter than the free-space wavelength: $\lambda_g \approx \frac{\lambda_0}{\sqrt{\varepsilon_{\text{eff}}}}$. For example, consider a laminate with relative permittivity $\varepsilon_r = 2{,}2$ and thickness $h = 0{,}254$ mm (typical value in mmWave, a compromise between bandwidth, losses). The patch width for the fundamental mode TM_{10} is estimated by the formula [5,6]:

$$W \approx \frac{c}{2f_0}\sqrt{\frac{2}{\varepsilon_r + 1}}. \tag{1}$$

After substituting $\frac{c}{2f_0} = \frac{3 \cdot 10^8}{2 \cdot 38 \cdot 10^9} \approx 3{,}95$ mm and $\sqrt{\frac{2}{3{,}2}} \approx 0{,}79$ we get $W \approx 3{,}12$ m . Then the effective permittivity is determined [5,6]:

$$\varepsilon_{\text{eff}} \approx \frac{\varepsilon_r + 1}{2} + \frac{\varepsilon_r - 1}{2}\left(1 + \frac{12h}{W}\right)^{-1/2}. \tag{2}$$

For $W/h \approx 3{,}12/0{,}254 \approx 12{,}3$ we have $12h/W \approx 0{,}98$, so $(1+12h/W)^{-1/2} \approx (1{,}98)^{-1/2} \approx 0{,}711$. We get $\varepsilon_{\text{eff}} \approx 1{,}6 + 0{,}6 \cdot 0{,}711 \approx 2{,}03$ The effective length of the resonator is [5-6]:

$$Leff \approx c2f0\varepsilon eff \approx 3{,}95 \text{ mm} 2{,}03 \approx 2{,}77 \text{ mm}. \tag{3}$$

 doi:10.20944/preprints202603.1927.v1

Due to the fringing fields, the resonator appears electrically longer. Therefore, a length correction ΔL is introduced, and the effective patch length is defined as$\approx L_{\text{eff}} - 2\Delta L$, where [5,6]:

$$\frac{\Delta L}{h} \approx 0{,}412 \cdot \frac{(\varepsilon_{\text{eff}} + 0{,}3)(W/h + 0{,}264)}{(\varepsilon_{\text{eff}} - 0{,}258)(W/h + 0{,}8)}. \quad (4)$$

After substitution $\varepsilon_{\text{eff}} \approx 2{,}03$ oraz $W/h \approx 12{,}3$ we get approximately $\Delta L/h \approx 0{,}52$, i.e., $\Delta L \approx 0{,}52 \cdot 0{,}254$ mm $\approx 0{,}132$ mm as a consequence $L \approx 2{,}77 - 2 \cdot 0{,}132 \approx 2{,}51$ mm. This means that a single patch at 38 GHz has dimensions of the order of a few millimeters (here approximately $W \approx 3{,}12$ mm and $L \approx 2{,}51$ mm), which clearly shows why multi-element integration (2 or 4 ports) is natural in mmWave frequencies—several radiating patches can be fitted on a small surface [5,6].

The next step involves feeding and impedance matching. For a microstrip line with a characteristic impedance of 50 Ω on a substrate with $\varepsilon_r = 2{,}2$i $h = 0{,}254$ mmthe trace width is on the order of fractions of a millimeter (typically around 0,7–0,8 mm, depending on the specific model used). Impedance matching to the patch is achieved using either an inset-feed or a quarter-wave transformer. In TM_{10} mode, the patch input resistance strongly depends on the distance from the feed point to the radiating edge; in simple terms, the feed point can be selected to achieve approximately 50 Ω at resonance, minimizing $|S_{11}|$ in the operating band. In 5G High-band, bandwidths of hundreds of MHz to several GHz are often required, so a single patch alone is often insufficient (it is naturally narrowband). Bandwidth may be enhanced by increasing the substrate thickness h, or by employing techniques such as slots, multi-resonant structures, stacked patches, and optimized radiator geometries. However, in mmWave designs, the laminate thickness cannot be excessively increased, as this leads to higher dielectric losses, the excitation of surface waves, and increased manufacturing complexity. Consequently, this paper focuses on bandwidth enhancement specifically through the modification of the radiator shape.

Once a single element is defined, we move on to a 2-element MIMO configuration. The simplest variant is two identical patches with two ports, spaced at a distance d. In practice, for mmWave, $d \approx 0{,}5\lambda_0$ is often assumed as the starting point for the trade-off between system gain and coupling, i.e., here $d \approx 0{,}5 \cdot 7{,}89$ mm $\approx 3{,}95$ mm. Such a small distance means that coupling can be significant, so the system often "breaks" symmetry: arranges the elements at an angle (e.g., one 90° rotation), uses orthogonal polarization, or introduces isolating elements in the ground plane. MIMO is not only about power summation as in a classic single-port array, but also about the lowest possible correlation between paths; However, in 5G mmWave, very often the same structures act as both MIMO and a small array antenna for beamforming, so parameters such as gain, beamwidth and sidelobe levels are also important.

For a 4-element configuration, the situation is similar, but the number of interactions increases. The four elements can be arranged linearly (1 × 4) or in a 2 × 2 matrix. The 2 × 2 arrangement is advantageous in compact devices because it provides two-dimensional beam control (in azimuth and elevation) and enables various MI-MO/beamforming strategies. Assuming a spacing of $d \approx 0{,}5\lambda_0$, a 2×2 array maintains a compact footprint with inter-element spacing of approximately 3.95 mm along both axes. When these four elements are driven independently, achieving high port isolation becomes critical, as each radiator in a 2×2 matrix has two immediate neighbors. From a MIMO performance perspective, the objective is to minimize the transmission coefficients ($|S_{21}|$, $|S_{31}|$, $|S_{41}|$) typically targeting values below −15 dB across the operating band, alongside a low Envelope Correlation Coefficient (ECC). Conversely, from an antenna theory standpoint, the goal is to maintain a robust realized gain for individual elements (several dBi) while ensuring a significant increase in array gain when the elements operate coherently.

To estimate the effect of the number of elements on the directivity, one can approximately consider the array factor. For a linear array of N elements with equal amplitudes and spacing d, with phase shift β (for beam scanning), the array factor has the form [17–19]:

 doi:10.20944/preprints202603.1927.v1

$$AF(\theta) = \sum_{n=0}^{N-1} e^{jn(kd\cos\theta+\beta)}, \quad (5)$$

where $k = 2\pi/\lambda_0$. For maximum "broadside" radiation, β=0 is assumed. Then, the gain increase compared to a single element, with perfect power summation and negligible losses, can be estimated as $10\log_{10}(N)$dB. This means that moving from 1 to 2 elements results in about 3 dB, and to 4 elements, about 6 dB of "system gain"—in practice, less due to power supply losses, matching imperfections, coupling, and packaging limitations. Nevertheless, at 38 GHz, even a few dB is valuable, as it directly translates to link budget and connection stability.

It is also essential to consider propagation losses, which justify the implementation of such high-gain systems. The Free-Space Path Loss (FSPL**)**, representing the reduction in power density as an electromagnetic wave propagates through space, can be calculated using the following formula: [17–20]:

$$FSPL(dB) = 20\log_{10}\left(\frac{4\pi R}{\lambda_0}\right). \quad (6)$$

For comparison, with $R = 100$ mi $\lambda_0 \approx 7{,}89$ mm we have$4\pi R/\lambda_0 \approx 4\pi \cdot 100/0{,}00789 \approx 1{,}59 \cdot 10^5$ so $FSPL \approx 20\log_{10}(1{,}59 \cdot 10^5) \approx 104$ dB. This shows that at 38 GHz the energy reserve quickly "disappears", so the antenna gain (e.g., obtained by a 2- or 4-element system) is a practical tool for maintaining the link, next to the transmitter power and receiver sensitivity.

In summary, 2-element and 4-element MIMO microstrip antennas are essential for 5G FR2 (38 GHz) applications, as they enable the integration of multiple radio paths within a highly constrained footprint. This configuration enhances throughput via spatial multiplexing and recovers a significant portion of the link budget through increased directivity and array gain. For a typical substrate ($\varepsilon_r \approx 2{,}2$, $h \approx 0{,}254$ mm), a single patch dimensions are approximately $W \approx 3{,}1$ mm and $L \approx 2{,}5$ mm, with an optimal inter-element spacing starting at $0{,}5\lambda_0 \approx 4$ mm—a critical compromise between mutual coupling mitigation and overall module size. Ultimately, the primary challenge in mmWave antenna design lies not in the basic patch geometry, but in the simultaneous optimization of impedance matching, operational bandwidth, and inter-port isolation within a millimeter-scale architecture that remains technologically feasible and stable inside a practical 5G device enclosure.

4. WAT Antenna Design for 38 GHz

Due to the planned frequency ranges of the 5G system, the main assumption for the designed antenna intended for this system is an operating frequency in the 38 GHz range (high-band). In addition to the frequency band, other important requirements for the designed antenna include antenna dimensions, which should be no larger than 10 × 10 mm, the highest possible energy gain, linear polarization, and the type of material from which the antenna is to be made. A professional laminate, ROGERS RT5880, was selected for the antenna design. This material has a thickness of h = 0.254 mm, an electrical permittivity of εr = 2.2, and low losses of tan(δ) = 0.0009. This substrate is a PTFE-based composite reinforced with glass microfibers, providing excellent chemical resistance, low moisture absorption, and ease of fabrication, which makes it a preferred choice for high-performance microstrip antennas.

A model was developed using the assumed antenna parameters in CST Microwave Studio microstrip antenna design software. This software also allows for determining the antenna's electrical parameters and radiation characteristics. Initially, the antenna design focused primarily on the S_{11} coefficient and the G gain. Finally, the CST Microwave Studio software optimized the resulting model to meet the antenna's requirements, modifying its dimensions and power supply. During the optimization process, the length and width of the antenna substrate with ground plane (Ws, We, Ls, Le), the length and width of the radiator (Lp, Wp), and the length and width of the feedline (Lf, Wf) were changed. Other structural elements, such as the thickness and permittivity of the substrate and the size of the letters "WAT," remained unchanged. The optimization process ultimately resulted in

 doi:10.20944/preprints202603.1927.v1

the antenna model shown in Figure 1, whose dimensions are presented in Table 1. For the resulting antenna model, a physical model of the antenna was created, the appearance of which is shown in Figure 2. Computer simulations and measurements were performed for the final model of the proposed antenna to determine the antenna's electrical parameters.

Table 1. Antenna design dimensions.

Antenna Component	Symbol	1 × 1 Antenna Dimensions [mm]	MIMO 2-elements Dimensions [mm]	MIMO 4-elements Dimensions [mm]
Substrate width	Ws	5.16	5.16	5.16
Substrate lenght	Ls	5.05	5.05	5.05
Ground plane width	We	5.16	-	-
Ground plane lenght	Le	5.05	-	-
Patch width	Wp	3.10	3.10	3.10
Patch lenght	Lp	2.06	2.06	2.06
Substrate thickness	H	0.254	0.254	0.254
Permitivity	ε_r	2.2	2.2	2.2
Feed line width	Wf	0.107	0.107	0.107
Feed line lenght	Lf	4.02	4.02	4.02
WAT letter height	Lw	1.00	1.00	1.00
WAT letter width	Ww	0.1	0.1	0.1
Substrate width	Wx	-	-	15.37
Substrate lenght	Lx	-	-	15.26
Substrate width	Wz	-	15.48	-
Substrate lenght	Lz	-	8.07	-

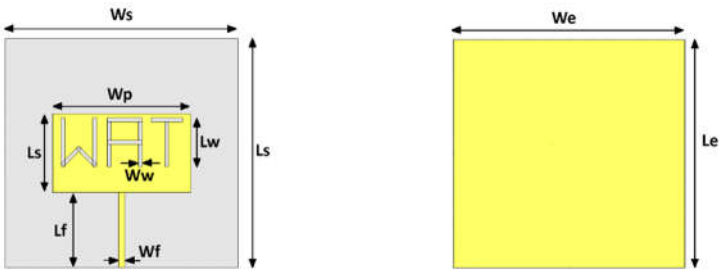

Figure 1. Microstrip antenna design with dimensions.

Figure 2. Appearance of the physical model of the proposed microstrip antenna.

5. MIMO WAT Antenna Designs for 38 GHz

Based on a single radiating element, the main design assumption was to create antennas designed for high-frequency operation (High-Band), particularly around 38 GHz. Antenna dimensions were also a significant design constraint. The overall dimensions of the antenna structure

 doi:10.20944/preprints202603.1927.v1

were assumed to be no larger than 25 × 25 mm, which meets the requirements of modern, compact radio modules used in user terminals, CPE (Customer Premises Equipment), and integrated mmWave modules. Limited space necessitates the use of microstrip technology and careful arrangement of the radiating elements, especially in the case of a 4-element MIMO configuration, where the problem of mutual electromagnetic coupling plays a key role.

Another important requirement was the highest possible antenna gain, achieved both through the appropriate design of a single radiating element and through the use of 2- and 4-element MIMO configurations. Multi-element structures assume the use of spatial phenomena to improve radiation characteristics and increase system efficiency in the context of 5G technology. Additionally, it was assumed that the designed antenna should be characterized by linear polarization, which is consistent with the requirements of many radio systems and facilitates integration with other elements of the transceiver chain.

Based on the presented assumptions and the developed single radiating element, two variants of microstrip antennas operating in the 38 GHz band were developed, differing in the number of radiating elements and system purpose. The first is a two-element MIMO antenna, representing a moderately complex solution intended for applications requiring compact dimensions and a limited number of transmitting and receiving paths. In this case, particular attention was paid to ensuring adequate impedance matching of both ports and achieving the lowest possible correlation between the elements, while maintaining a compact size of the entire antenna structure.

The second variant is a 4-element MIMO antenna configuration, designed for applications requiring higher data throughput and improved spectral efficiency, typical of 5G FR2 (High-Band) systems. Increasing the number of radiating elements enables the implementation of advanced transmission techniques, such as spatial multiplexing and beamforming, but also entails a substantial escalation in design complexity. For the 4-element structure, the primary challenge was mitigating mutual electromagnetic coupling between adjacent elements and maintaining high port-to-port isolation within an extremely limited available footprint. The developed MIMO antenna models are shown in Figure 3, with their specific dimensions detailed in Table 1. Subsequently, physical prototypes were fabricated, as illustrated in Figure 4.

Both MIMO antenna variants were designed based on the same single microstrip element, enabling direct comparison of the effect of the number of elements on antenna parameters such as operating bandwidth, realized gain, radiation characteristics, and MIMO metrics. Adopting a uniform manufacturing technology and a common dielectric substrate also allows for an objective assessment of the trade-offs between structure complexity and achieved system benefits. The developed 2- and 4-element MIMO configurations thus provide a starting point for further simulation analyses and comparisons aimed at assessing the suitability of the designed antennas for applications in modern 5G systems operating in the millimeter-wave band.

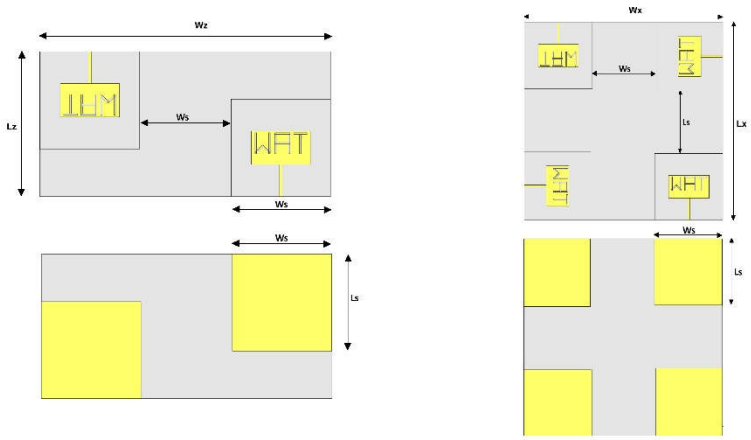

Figure 3. MIMO 2 and MIMO 4 microstrip antenna design with dimension markings.

 doi:10.20944/preprints202603.1927.v1

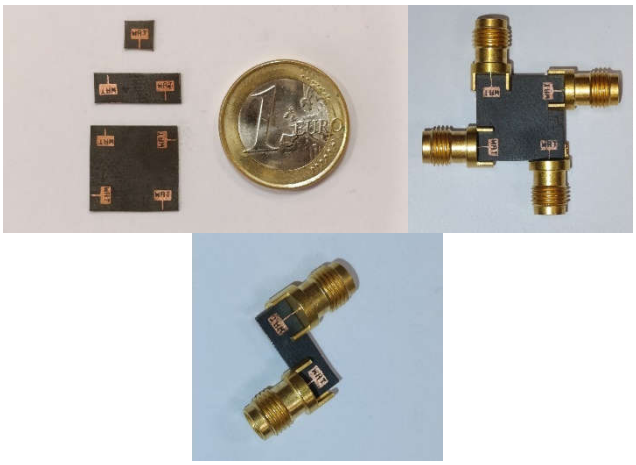

Figure 4. The view of the physical models of MIMO 2 and MIMO 4 microstrip antennas.

6. Simulation and Measurement Results for the Developed Models

The proposed antenna structures, designed for 5G mmWave and future 6G applications, are implemented as planar microstrip patch antennas. Each configuration consists of three fundamental layers: a ground plane, a radiating element (patch), and a dielectric substrate that acts as both a mechanical carrier and a medium influencing the electromagnetic propagation characteristics. Precise optimization of the radiator's geometric parameters, the ground plane dimensions, and the substrate's dielectric properties (permittivity and loss tangent) is essential to achieving the desired resonant behavior and impedance bandwidth within the targeted millimeter-wave frequency range.

Based on the single radiating element design, multi-element configurations were also developed, including a single-element antenna (SI-SO) as the basic radiating module, as well as 2-element MIMO and 4-element MIMO structures. In the MIMO configuration, the radiating elements were arranged to ensure adequate isolation between antenna ports and to limit mutual electromagnetic coupling between individual elements. This is crucial for the correct operation of MIMO systems, which require high radio channel independence and appropriate diversity properties.

The design and optimization of antenna parameters was carried out using the CST Microwave Studio simulation environment, which allows for full-wave analysis of the electromagnetic field distribution within the antenna structure. During the simulation phase, the influence of the antenna's geometric parameters on its frequency response and radiation properties was analyzed.

To verify the simulation results, experimental measurements of selected electrical parameters were also performed using a Rohde & Schwarz ZVA67 vector network analyzer. During the measurements, reflection coefficients and transmission coefficients were determined, which are the basic parameters determining the impedance matching of the antenna to the feed path and the coupling between the antenna ports. The appearance of the designed antenna during reflection coefficient measurements is shown in Figure 5.

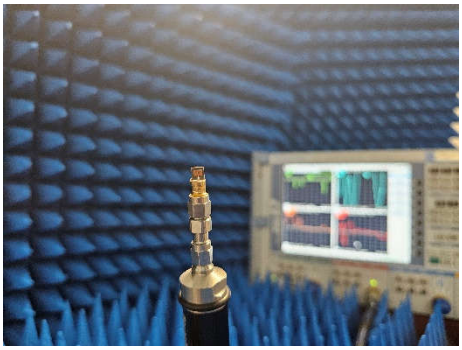

Figure 5. The view of the completed microstrip antenna connected to the ZVA67 network analyzer during measurements.

 doi:10.20944/preprints202603.1927.v1

As a result of the numerical simulations and laboratory measurements, the characteristics of the basic electrical parameters describing the properties of the designed antenna structures were obtained.

All obtained results were compiled and compared to perform a detailed analysis of the properties of the designed microstrip antenna in a single-element configuration and in MIMO structures with two and four elements. Comparison of simulation results with measurement results allows for the assessment of the correctness of the adopted numerical model and verification of their suitability for modern telecommunications systems operating in the 5G mmWave and 6G bands.

6.1. Reflection and Transmission Coefficient

In MIMO (Multiple-Input Multiple-Output) antennas, scattering parameters (S-parameters) are used to describe the electrical properties. One of the most important is the reflection coefficient, designated as S_{11}, S_{22}, etc., which determines the degree of impedance matching of the antenna to the feed path (usually 50 Ω). This parameter indicates how much of the power fed to the antenna port is reflected back to the feed line due to impedance mismatch. In practice, proper antenna matching is assumed to occur when the reflection coefficient is less than −10 dB, meaning that most of the energy is effectively transferred to the antenna and radiated. Analysis of the reflection and transmission coefficients allows us to assess both the impedance matching of individual antenna elements and the level of interaction between elements in multi-antenna structures, which is crucial for the efficiency of wireless communication systems. Figure 6 below shows the input port numbers of the designed antennas, for which simulations and measurements of the reflection and transmission coefficients were performed.

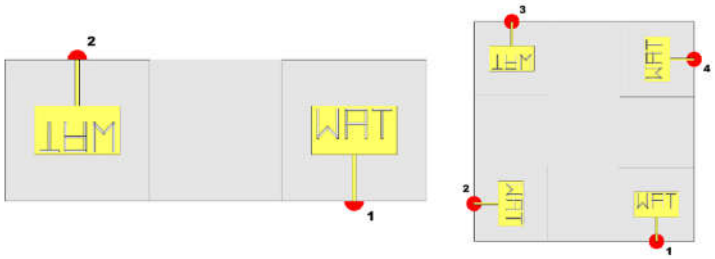

Figure 6. Proposed numbering of input ports of the designed MIMO antennas.

Figure 7 shows the simulation results and the reflection coefficient measurement results for the proposed 1 × 1 (SISO), 2-element MIMO and 4-element MIMO antennas.

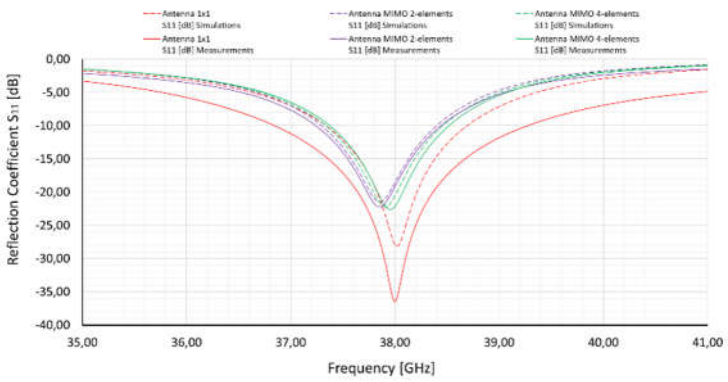

Figure 7. The value of the S11 reflection coefficient as a function of frequency for the proposed antennas.

For all analyzed structures, a clear resonance is observed near a frequency of approximately 38 GHz, where the reflection coefficient value reaches a minimum. The best impedance matching is demonstrated by the single-element antenna, for which the minimum S_{11} w value in the simulation

 doi:10.20944/preprints202603.1927.v1

reaches approximately −36 dB, while in the measurements it reaches approximately −27 dB. This indicates a very good match of the antenna to the feedline and high efficiency of power transfer to the radiator. The slight difference between the simulation and measurement results is likely due to inaccuracies in the structure's manufacturing, tolerances in the substrate material parameters, and the influence of the measurement connector.

For the 2-element MIMO and 4-element MIMO configurations, slightly higher reflection coefficient values are observed at the resonant point (around −20 dB to −23 dB), which is typical for multi-antenna structures. This is due to mutual electromagnetic coupling between the radiating elements, which can slightly degrade impedance matching. Despite this, the S_{11} values remain well below −10 dB, confirming the correct matching of all designed antenna configurations. The operating bandwidth for all structures is greater than 400 MHz, allowing the proposed antennas to be used in 5G high-band applications.

A comparison of the simulation and measurement results shows good agreement between the characteristics, while also showing a slight shift and shallower resonance minimum in the measurement results. This demonstrates the validity of the adopted simulation model and confirms that the designed antennas—both the single-element antenna and the 2-element MIMO and 4-element MIMO configurations—can operate effectively in the designed frequency band of approximately 38 GHz.

The second important parameter is the transmission coefficient, most often denoted as S_{21}, S_{12}, S_{31}, etc., which describes the level of signal penetration between individual antenna ports. In MIMO structures, this parameter determines the degree of electromagnetic coupling between radiating elements and the level of isolation between them. Low values of the transmission coefficient (e.g., below −15 dB or −20 dB) indicate good isolation between antenna elements, which is important for ensuring the independence of transmission channels and the proper operation of MIMO systems. Figure 8 presents the characteristics of the transmission coefficient between the antenna ports as a function of frequency for the 2-element MIMO and 4-element MIMO structures, obtained both from simulation and measurements. For the 2-element MIMO and 4-element MIMO antennas, the S_{21} parameter is analyzed. Additionally, for the 4-element MIMO antenna, the S_{31} parameter, which describes the coupling between the antenna elements positioned at 90 degrees to each other, is also presented. The measurement and simulation results for both reflection coefficients and transmission coefficients at individual ports are similar. For clarity, only values for selected ports are shown in Figure 8. S_{21} represents the transmission coefficient for ports with the same power line polarity, and S_{31} represents the transmission coefficient for ports with the power lines offset by 90 degrees.

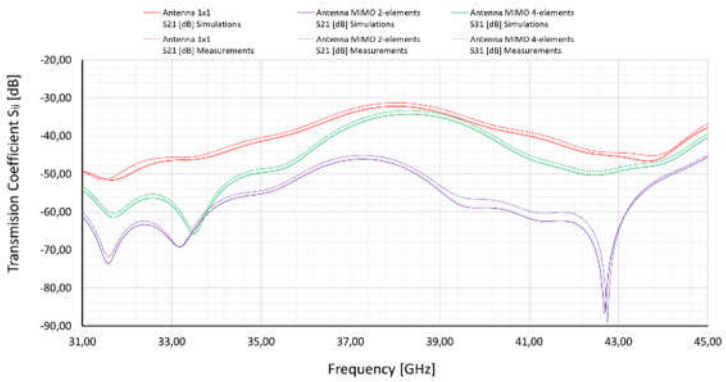

Figure 8. The value of transmission coefficients of the proposed MIMO antennas as a function of frequency.

In the 2-element MIMO configuration, the S_{21} transmission coefficient typically varies between −30 dB and −50 dB over the majority of the analyzed frequency range. A marginal increase in the transmission coefficient—reaching roughly −30 dB—is noted near the 38 GHz resonance. This behavior is expected at the operating frequency, as electromagnetic radiation is most effective in this region. Nevertheless, the mutual coupling remains low, confirming high isolation between the ports.

 doi:10.20944/preprints202603.1927.v1

For the 4-element MIMO setup, the transmission coefficients exhibit even greater suppression. The S_{21} parameter reaches values of roughly −35 dB, whereas S_{31} —characterizing the coupling between non-adjacent elements—drops below −45 dB across the operating frequency range. Such results confirm superior isolation and minimal mutual coupling between the individual ports of the antenna array.

Comparison of the simulation and measurement results indicates good agreement of the characteristics, although small amplitude differences may result from inaccuracies in the structure's manufacturing, tolerances in the substrate's material parameters, and the influence of measurement connectors. The obtained transmission coefficient values, significantly lower than -20 dB, confirm very good isolation between the antenna ports, which is an important condition for the proper operation of MIMO systems in the millimeter wave band.

6.2. Input Impedance

Antenna input impedance is a complex quantity consisting of a real (resistive) part and an imaginary (reactant) part, whose values vary as a function of frequency. In MIMO structures, this parameter is analyzed separately for each antenna port, because each radiating element has its own feed path. The designed antennas assume a feed line impedance of 50 Ω, which is a standard value used in microwave systems and measurement systems.

Appropriate selection of the width and length of the microstrip feedlines allowed for proper impedance matching of the individual antenna elements. As a result, within the operating band of the designed structures—for both the single-element antenna and the 2-element MIMO and 4-element MIMO configurations—input impedance values close to the nominal value of approximately $Z_0 \approx 50\ \Omega$ were achieved, with a very small imaginary component. This means that the energy delivered to the antenna ports is efficiently transferred to the radiating elements, and losses resulting from impedance mismatch are minimal.

Detailed characteristics of the input impedance of individual antenna ports as a function of frequency are presented in Figure 9, which allows for the assessment of the quality of impedance matching in the analyzed operating band of the proposed antenna structures.

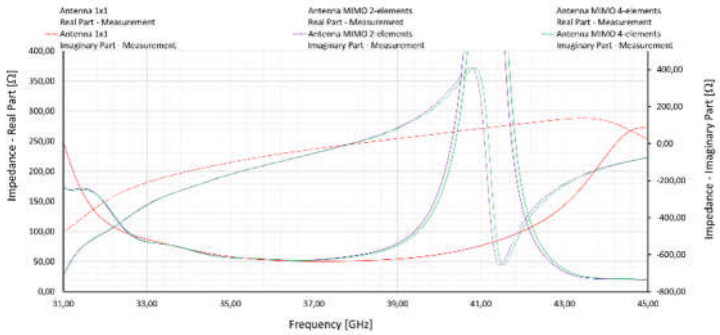

Figure 9. Input impedance value for the proposed MIMO antennas.

6.3. Antenna Gain

One of the important parameters analyzed when designing microstrip antennas operating in MIMO configurations is the antenna's energy gain. This parameter determines the antenna's ability to effectively radiate electromagnetic energy in a specific direction relative to an isotropic antenna and is expressed in dBi. In multi-antenna structures, the energy gain is analyzed for individual radiating elements, as each of them constitutes an independent antenna port in the MIMO system. The situation is different for antenna arrays, which are considered as a single antenna system with a resultant radiation pattern. A properly designed arrangement of radiating elements should provide stable gain values within the operating band while maintaining favorable radiation properties and adequate isolation between antenna elements.

 doi:10.20944/preprints202603.1927.v1

Figure 10 shows the antenna gain versus frequency curves for the three analyzed configurations: a single-element antenna, a 2-element MIMO antenna, and a 4-element MIMO antenna, obtained both from simulation and measurements. In the analyzed antenna operating band range from approximately 37 GHz to 39 GHz, the energy gain values for all structures remain at a similar level. For a single-element antenna, the gain is approximately 7.3–7.5 dBi, while for the 2-element MIMO and 4-element MIMO configurations, slightly lower values are observed outside the operating band, ranging from approximately 6.0 to 7.4 dBi. A slight reduction in gain in multi-antenna structures is typical and results primarily from the presence of additional radiating elements and electromagnetic interactions between them. This phenomenon occurs outside the operating band of the proposed antennas.

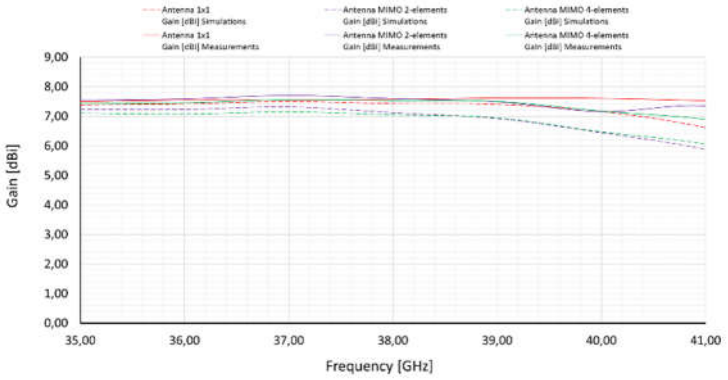

Figure 10. The value of the antenna gain for the proposed MIMO antennas.

A comparison of the simulation and measurement results indicates good agreement between the obtained characteristics, with a slight decrease in the energy gain for MIMO structures observed in the higher part of the analyzed band. This may be due to inaccuracies in the antenna structure's manufacturing, tolerances in the substrate material parameters, and the influence of the measurement elements. Nevertheless, the obtained energy gain values can be considered satisfactory, as they remain relatively stable throughout the antenna's operating band, confirming the correctness of the designed antenna structures and their suitability for wireless communication systems operating in the millimeter-wave band.

6.4. The Radiation Pattern

The radiation pattern describes the way electromagnetic energy emitted by an antenna propagates in space, depending on its direction. It represents the normalized distribution of electric field strength or the relative distribution of the surface power density radiated by the antenna. In MIMO structures, radiation patterns are analyzed for individual radiating elements, as each element constitutes an independent antenna port. Analysis of these patterns allows for the assessment of radiation directionality, main beam width, and sidelobe level, which is crucial for transmission efficiency in multi-antenna systems.

Figure 11 presents three-dimensional (3D) radiation patterns of the designed antennas for a selected frequency within the operating band, i.e., 38 GHz, obtained from simulations conducted in the CST Microwave Studio environment. Figures 12 and 13 present the measured normalized radiation patterns of the proposed MIMO antennas in the vertical (V) and horizontal (H) planes, respectively, for frequencies of 37.5 GHz, 38 GHz, and 38.5 GHz.

Analysis of the presented characteristics indicates that the radiation pattern of the proposed antennas remains stable and repeatable over a wide frequency range. This means that for both the single-element antenna and the 2-element MIMO and 4-element MIMO configurations, the antenna structure maintains similar radiation characteristics across the entire operating band analyzed. The obtained results confirm the correctness of the designed antenna geometry and indicate its good

 doi:10.20944/preprints202603.1927.v1

radiation properties, which is particularly important in broadband wireless communication systems operating in the millimeter wave band.

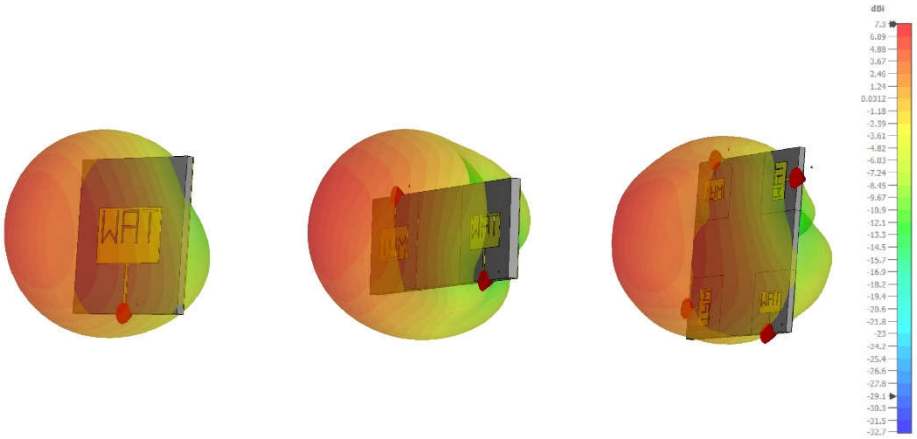

Figure 11. 3D radiation patterns of the proposed MIMO antennas for 38 GHz.

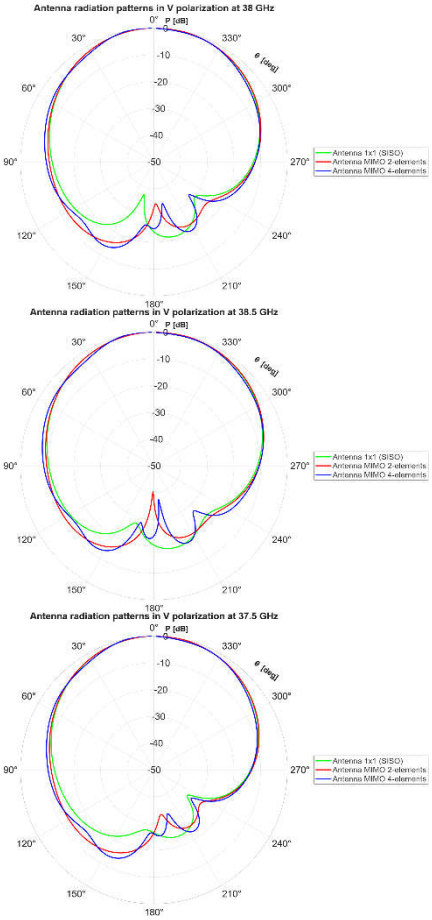

Figure 12. Measured normalized radiation patterns of the proposed MIMO antennas in the vertical V plane at 37.5 GHz, 38 GHz, 38.5 GHz.

 doi:10.20944/preprints202603.1927.v1

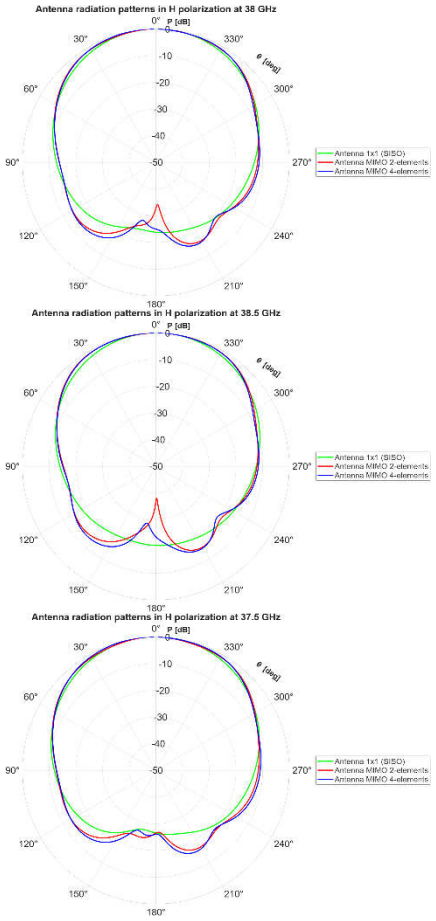

Figure 13. Measured normalized radiation patterns of the proposed MIMO antennas in the vertical H plane at 37.5 GHz, 38 GHz, 38.5 GHz.

6.5. Envelope Correlation Coefficient (ECC) i Diversity Gain (DG)

The analysis of radiation pattern allows for the assessment of the antenna's radiation properties and its behavior in different spatial directions, which is particularly important in the case of MIMO structures, where each antenna element constitutes a separate transmission port.

In order to assess the performance of the multi-antenna system, additional parameters describing the antenna diversity properties, such as the Envelope Correlation Coefficient (ECC) and Diversity Gain (DG), were also analyzed. The ECC coefficient determines the degree of correlation between signals received by individual antenna elements and can be determined based on the antenna dispersion parameters according to the relationship [21–25]:

$$ECC = \frac{|\, S_{11}^{*}S_{12} + S_{21}^{*}S_{22} \,|^2}{(1-|\, S_{11} \,|^2 - |\, S_{21} \,|^2)(1-|\, S_{22} \,|^2 - |\, S_{12} \,|^2)}. \quad (7)$$

Whereas the diversification profit DG is calculated on the basis of the ECC coefficient in accordance with the relationship [21–25]:

$$DG = 10\sqrt{1 - ECC} \quad (8)$$

In MIMO systems, very low ECC values and high Diversity Gain (DG) values are desirable, as this indicates low correlation between antenna elements and high independence of transmission channels. For the proposed four-port MIMO antenna, very favorable values of these parameters were obtained—ECC of approximately 0.00001 and DG of approximately 10 dB. Such a low correlation coefficient value indicates very good isolation between antenna elements and high efficiency of the MIMO system, which confirms the usefulness of the designed antenna structures in modern wireless

 doi:10.20944/preprints202603.1927.v1

communication systems. Figure 14 presents the determined ECC and Div. Gain values for the developed 2-element MIMO and 4-element MIMO antennas.

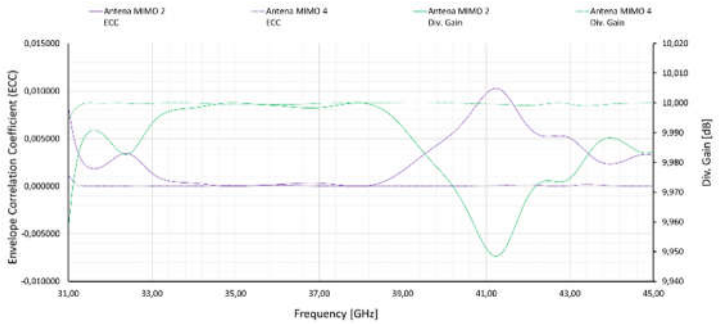

Figure 14. ECC and Div. Gain Values for the Proposed MIMO Antennas.

The figure shows the envelope correlation coefficient (ECC) and diversity gain (DG) as a function of frequency for the designed configurations of a 2-element MIMO antenna and a 4-element MIMO antenna. These parameters are important indicators for assessing the performance of multi-antenna systems because they describe the degree of independence of signals received by individual radiating elements.

For the ECC coefficient, very low values are observed across the entire analyzed frequency band from approximately 31 GHz to 45 GHz. The antenna operating point near 38 GHz is particularly important, where the ECC values for both MIMO configurations are close to zero and do not exceed approximately 0.0000001. Such low values indicate very little correlation between the antenna elements, meaning that the individual antenna ports operate largely independently. This is a desirable feature in MIMO systems, as it enables effective use of diversity techniques and increases the throughput of the communication system.

In turn, the diversity gain for both analyzed configurations remains close to 10 dB across the entire frequency range. In particular, for the 38 GHz frequency, the DG values are approximately 9.98–10 dB, which is very close to the theoretical maximum value for MIMO systems. Such a high level of diversity gain confirms that the designed antennas provide high signal diversity efficiency and good performance in multi-antenna structures.

Based on the analysis of the figure, it can be concluded that both the 2-element MIMO antenna and the 4-element MIMO antenna meet the requirements of modern MIMO systems. Low ECC values and DG values close to 10 dB at the 38 GHz operating frequency confirm very good isolation between the antenna elements and the high performance of the multi-antenna system.

6.5. Channel Capacity Loss (CCL)

Another important parameter used to evaluate the performance of multiport antennas is Channel Capacity Loss (CCL). This parameter measures the reduction in the maximum capacity of a transmission channel caused by the antenna's properties during transmission and receptionIn practice, it is assumed that the correct operation of a MIMO antenna is ensured when the CCL value is less than 0.4 bit/s/Hz. The CCL coefficient values for the designed MIMO antenna were determined based on the dispersion parameters and are presented in Figure 15. As a result of the conducted analyses, a CCL value of approximately 0.008 bit/s/Hz was obtained, which is significantly lower than the permissible limit and indicates a very small loss of channel capacity.

The CCL coefficient is determined according to the relationship [25–29]:

$$CCL = -\log_2 \det(\alpha_R), \tag{9}$$

where α_R is defined as:

 doi:10.20944/preprints202603.1927.v1

$$\alpha_R = \begin{bmatrix} \alpha_{11} & \alpha_{12} \\ \alpha_{21} & \alpha_{22} \end{bmatrix} \quad (10)$$

The elements of this matrix are calculated based on the antenna dispersion parameters according to the relationship:

$$\alpha_{ii} = 1 - |\sum_{n=1}^{2} S_{in} S_{ni}| \quad (11)$$

$$\alpha_{ij} = -|\sum_{n=1}^{2} S_{in} S_{nj}| \quad (12)$$

where S_{ij} o are marked by the corresponding elements of the dispersion parameter matrix. The very low CCL value obtained for the designed antenna indicates high signal transmission efficiency in the MIMO system and also confirms good isolation between the antenna ports and a low level of correlation between the radiating elements [25–29].

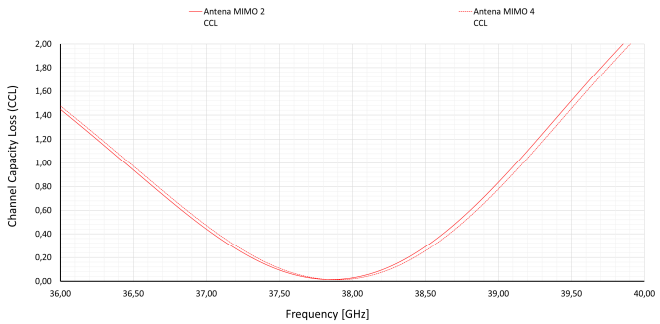

Figure 15. CCL values for the proposed MIMO 2 and MIMO 4 antennas.

7. Conclusions

This article presents the concept and analysis of microstrip antennas designed for operation in the millimeter wave band, developed in three configurations: a single-element antenna (SISO 1×1) and MIMO 2-element and MIMO 4-element structures. The proposed solution was designed for applications in modern wireless communication systems, particularly in 5G networks using mmWave bands, where high transmission throughput, low latency, and the ability to support a large number of users are required.

The use of microstrip technology allows for a compact, lightweight, and easy-to-integrate antenna structure that can be directly implemented in modern telecommunications devices. These antennas are also characterized by low production costs, simple design, and easy integration with microwave systems, making them an attractive solution for mobile devices, user terminals, wireless access systems, and network infrastructure.

A particular advantage of the proposed design is its ability to be used in multi-antenna MIMO configurations, which are a key element of 5G technology. The use of multiple radiating elements enables the use of spatial diversity and spatial multiplexing techniques, which leads to increased transmission system capacity, improved connection reliability, and better utilization of the available frequency band. MIMO antennas also enable more effective countermeasures against multipath signal propagation and interference in the radio environment.

A significant advantage of the proposed antenna is the improvement in selected electrical parameters compared to many existing microstrip antenna designs used in similar applications. The developed structure is characterized by increased energy gain, stable radiation properties over a wide frequency range, and favorable operating parameters in multi-antenna configurations. High isolation

 doi:10.20944/preprints202603.1927.v1

between the radiating elements and good diversity properties enable the proposed antenna to effectively support data transmission in systems using MIMO techniques.

Another important feature of the proposed design is its scalability, enabling the use of a single antenna element in both single-port configurations and more complex multi-antenna systems. This approach allows for easy adaptation of the antenna architecture to various applications—from simple communication devices to advanced network infrastructure systems and solutions requiring a large number of antenna elements, such as massive MIMO systems.

From a practical application perspective, 5G networks can benefit from antennas of this type in a variety of applications, including base stations, access points, user terminals, short-range wireless communication systems, and very high-bandwidth transmission systems. Operating in the millimeter-wave band allows for the use of wide transmission bandwidths, which translates into significant increases in data transfer rates and improved spectral efficiency of communication systems.

In summary, the proposed microstrip antenna design in SISO, MIMO 2-element, and MIMO 4-element configurations is a promising solution for modern wireless communication systems. Its compact design, ability to integrate with electronic circuits, increased energy gain, favorable performance parameters, and compatibility with multi-antenna technologies make it widely applicable in developing 5G mmWave systems, as well as in future generations of wireless networks.

Author Contributions: Conceptualization, R.P. and M.B; methodology, R.P.; software, K.B.; validation, R.P. and M.B; resources, ALL; data curation, M.B. and K.B.; writing—original draft preparation, R.P.; writing—review and editing, M.B. and K.B.; visualization, R.P. and M.B; project administration, R.P.; funding acquisition, All authors have read and agreed to the published version of the manuscript.

Funding: This work was financed by Military University of Technology under research project UGB/22-124/2026/WAT entitled "Testing of radiated emission disturbances of selected smartphones using an anechoic chamber and an OTEM chamber in the aspect of the requirements of the PN-EN 17025 standard".

Institutional Review Board Statement: Not applicable.

Informed Consent Statement: Not applicable.

Data Availability Statement: Data available on request due to legal restrictions.

Conflicts of Interest: The authors declare no conflicts of interest.

Abbreviations

The following abbreviations are used in this manuscript:

MIMO	Multiple Input Multiple Output
5G NR	5G New Radio
LOS	Line Of Sight
FSLP	Free Space Lose Path
ECC	Envelope Correlation Coefficient
DG	Diversity Gain
CPE	Customer Premises Equipment
CCL	Channel Capacity Loss

References

1. S. Parkvall, E. Dahlman, A. Furuskar, and M. Frenne, "NR: The new 5G radio access technology," *IEEE Communications Standards Magazine*, vol. 1, no. 4, pp. 24–30, Dec. **2017**, doi: 10.1109/MCOMSTD.2017.1700042.
2. A. P. Prakusya, D. A. Nurmantris, and R. A. -, " 4 Element MIMO Antenna For 5G Communications at 3.5 GHz Frequency," *Jurnal Rekayasa Elektrika*, vol. 18, no. 3, Sep. **2022**, doi: 10.17529/jre.v18i3.26673.

 doi:10.20944/preprints202603.1927.v1

3. Icmez, B.O.; Kurnaz, C. High-Gain Dual-Band Microstrip Antenna for 5G mmWave Applications: Design, Optimization, and Experimental Validation. *Appl. Sci.* **2025**, *15*, 3993. https://doi.org/10.3390/app15073993.
4. Icmez, B.O.; Kurnaz, C. High-Gain Dual-Band Microstrip Antenna for 5G mmWave Applications: Design, Optimization, and Experimental Validation. *Appl. Sci.* **2025**, *15*, 3993. https://doi.org/10.3390/app15073993.
5. Przesmycki, R.; Bugaj, M. Crescent Microstrip Antenna for LTE-U and 5G Systems. *Electronics* **2022**, *11*, 1201. https://doi.org/10.3390/electronics11081201.
6. Przesmycki, R.; Bugaj, M.; Nowosielski, L. Broadband Microstrip Antenna for 5G Wireless Systems Operating at 28 GHz. *Electronics* **2021**, *10*, 1. https://doi.org/10.3390/electronics10010001.
7. Bhadravathi Ghouse, P.S.; Kumar, P.; Mane, P.R.; Pathan, S.; Ali, T.; Boulogeorgos, A.-A.A.; Anguera, J. Dual-Band Antenna at 28 and 38 GHz Using Internal Stubs and Slot Perturbations. *Technologies* **2024**, *12*, 84. https://doi.org/10.3390/technologies12060084.
8. Hussain, S.A.; Taher, F.; Alzaidi, M.S.; Hussain, I.; Ghoniem, R.M.; Sree, M.F.A.; Lalbakhsh, A. Wideband, High-Gain, and Compact Four-Port MIMO Antenna for Future 5G Devices Operating over Ka-Band Spectrum. *Appl. Sci.* **2023**, *13*, 4380. https://doi.org/10.3390/app13074380.
9. S. Singh, A. Kumar Singh, Karunesh, A. Pandey, and R. Singh, "A Novel MIMO Microstrip Patch Antenna for 5G Applications,"in Proceedings—IEEE 2021 International Conference on Computing, Communication, and Intelligent Sistems, ICCCIS **2021**, *Institute of Electrical and Electronics Engineers Inc., Feb. 2021*, pp. 828–833. doi: 10.1109/ICCCIS51004.2021.9397137.
10. S. Parkvall, E. Dahlman, A. Furuskar, and M. Frenne, "NR: The new 5G radio access technology," *IEEE Communications Standards Magazine*, vol. 1, no. 4, pp. 24–30, Dec. **2017**, doi: 10.1109/MCOMSTD.2017.1700042.
11. H. Al-Saif, M. Usman, M. T. Chughtai, and J. Nasir, "Compact Ultra-Wide Band MIMO Antenna Sistem for Lower 5G Bands," *Wirel Commun Mob Comput*, vol. 2018, **2018**, doi: 10.1155/2018/2396873.
12. W. Zhang, Z. Weng, and L. Wang, "Design of a dual-band MIMO antenna for 5G smartphone application," in *2018 International Workshop on Antenna Technology (iWAT)*, **2018**, pp. 1–3. doi: 10.1109/IWAT.2018.8379211.
13. Kikan, V.; Bano, T.; Bhardwaj, S.; Kumar, A.; Sharma, M. A Comparative Review on Theory and Designing of 28/38 GHz 5G MIMO and Array Antenna. *In Proceedings of the 2023 International Conference on Innovative Data Communication Technologies and Application (ICIDCA)*, Uttarakhand, India, 14–16 March **2023**; pp. 1014–1020.
14. Raj, T.; Mishra, R.; Kumar, P. Advances in MIMO Antenna Design for 5G: A Comprehensive Review. Sensors **2023**, 23, 6329.
15. Hamdan, N.; Kurnaz, Ç. A Novel Dual-Band Four Port MIMO Antenna Design for 28/38 GHz Millimeter-Wave 5G Applications. *Balkan J. Electr. Comput. Eng.* **2024**, 12, 273–281.
16. Nayak, A.; Dutta, S.; Mandal, S. Design of Dual Band Microstrip Patch Antenna for 5G Communication Operating at 28 GHz and 46 GHz. *Int. J. Wirel. Microw. Technol.* **2023**, 13, 43–52.
17. Esmail, B.A.F.; Koziel, S. Design and Optimization of Metamaterial-Based Dual-Band 28/38 GHz 5G MIMO Antenna with Modified Ground for Isolation and Bandwidth Improvement. *IEEE Antennas Wireless Propag. Lett.* **2022**, 22, 1069–1073.
18. A. Hindi, E. Trrad and M. Dwairi, "A Compact 2 × 1 MIMO MicrostripPatch Antenna with Enhanced Gain for UWB Applications," *2023IEEE Jordan International Joint Conference on Electrical Engineeringand Information Technology (JEEIT)*, Amman, Jordan, **2023**, pp. 255–258, doi: 10.1109/JEEIT58638.2023.10185806.
19. Ahmed, H.; Ameen, A.M.; Magdy, A.; Nasser, A.; Abo-Zahhad, M. Slotted Circular-Patch MIMO Antenna for 5G Applications at Sub-6 GHz. *Telecom* **2025**, *6*, 53. https://doi.org/10.3390/telecom6030053.
20. Tiwari, R.N.; Thirumalaiah, R.; Naidu, V.R.; Sreenivasulu, G.; Singh, P.; Rajasekaran, S. Compact dual-band 4-port MIMO antenna for 5 G-sub 6 GHz/N38/N41/N90 and WLAN frequency bands. *AEU-Int. J. Electron. Commun.* **2023**, 171, 154919.
21. Din, I.U.; Alibakhshikenari, M.; Virdee, B.S.; Ullah, S.; Ullah, S.; Akram, M.R.; Ali, S.M.; Livreri, P.; Limiti, E. High-performance antenna system in MIMO configuration for 5G wireless communications over sub-6 GHz spectrum. *Radio Sci.* **2023**, 58, 1–22.

 doi:10.20944/preprints202603.1927.v1

22. Shamoon, S.; Zhou, W.Y.; Shahzad, F.; Ali, W.; Subbyal, H. Integrated sub-6 GHz and millimeter wave band antenna array modules for 5G smartphone applications. *AEU-Int. J. Electron. Commun.* **2023**, 161, 154542.
23. Khan, S.; Marwat, S.N.K.; Khan, M.A.; Ahmed, S.; Gohar, N.; Alim, M.E.; Algarni, A.D.; Elmannai, H. A Self-Decoupling Technique to Realize Dense Packing of Antenna Elements in MIMO Arrays for Wideband Sub-6 GHz Communication Systems. *Sensors* **2023**, 23, 654.
24. John, D.M.; Vincent, S.; Pathan, S.; Shinde, K.D.; Supreetha, B.S.; Ali, T. Eight-Element Flexible MIMO Antenna Based on Characteristics Mode Theory with Enhanced Channel Capacity for Sub 6 GHz 5G Communications. *Results Eng.* **2025**, 25, 104208.
25. Xiaoming Chen; Ping Jack Soh; Mohammad S. Sharawi, "Measurement Methods for MIMO Antenna Systems," in *MIMO Antenna Systems for 5G and Beyond* , IEEE, **2025**, pp.323-370, doi: 10.1002/9781119932543.ch9.
26. Lin, C.-W.; Chung, M.-A.; Chuang, B.-R. On-Chip Yagi Antenna Design at 38 GHz with 0.18 μm CMOS Techniques. *Electronics* **2025**, *14*, 4373. https://doi.org/10.3390/electronics14224373.
27. Alsaab, N.; Shaban, M. Design and Realization of a Multi-Band, High-Gain, and High-Isolation MIMO Antenna for 5G mmWave Communications. *Appl. Sci.* **2025**, *15*, 6857. https://doi.org/10.3390/app15126857.
28. Ibrahim, A.A.; Ali, W.A.E.; Alathbah, M.; Sabek, A.R. Four-Port 38 GHz MIMO Antenna with High Gain and Isolation for 5G Wireless Networks. *Sensors* **2023**, *23*, 3557. https://doi.org/10.3390/s23073557.
29. Xiaoming Chen; Ping Jack Soh; Mohammad S. Sharawi, "MIMO Antenna Fundamentals and Characterization Methods," in *MIMO Antenna Systems for 5G and Beyond* , IEEE, **2025**, pp.13-40, doi: 10.1002/9781119932543.ch2.